Calibration of Multi-region MFD Models using Mobile Phone Data

Mahendra Paipuri, Yanyan Xu, Marta C Gonzalez, Ludovic Leclercq

▶ **To cite this version:**

Mahendra Paipuri, Yanyan Xu, Marta C Gonzalez, Ludovic Leclercq. Calibration of Multi-region MFD Models using Mobile Phone Data. hEART 2020, 9th Symposium of the European Association for Research in Transportation - Virtual conference, Feb 2021, Lyon, France. 12p. hal-03154878

HAL Id: hal-03154878
https://hal.science/hal-03154878v1

Submitted on 1 Mar 2021

HAL is a multi-disciplinary open access archive for the deposit and dissemination of scientific research documents, whether they are published or not. The documents may come from teaching and research institutions in France or abroad, or from public or private research centers.

L'archive ouverte pluridisciplinaire **HAL**, est destinée au dépôt et à la diffusion de documents scientifiques de niveau recherche, publiés ou non, émanant des établissements d'enseignement et de recherche français ou étrangers, des laboratoires publics ou privés.

Calibration of Multi-region MFD Models using Mobile Phone Data

Mahendra Paipuri[1], Yanyan Xu[2], Marta C. González[2] & Ludovic Leclercq[1]

[1]Univ. Gustave Eiffel, Univ. Lyon, ENTPE, LICIT, F-69518, Lyon, France
{mahendra.paipuri, ludovic.leclercq}@univ-eiffel.fr
[2]Department of Civil and Environmental Engineering, University of California, Berkeley, CA, 94720, USA
{yanyanxu, martag}@berkeley.edu

Manuscript submitted for presentation at the hEART 2020 9th Symposium
Sept. 1–3, 2020, Lyon, France

Word count: 2941 words (excluding the references)
February 11, 2020

Abstract

The present work proposes a framework to calibrate MFD models using mobile phone data. The three major components to calibrate in the present context include MFD shape, regional trip lengths and path flow distribution. Time dependent penetration rates are estimated by fusing the OD matrix and the Loop Detector Data (LDD). The estimated MFDs are stable with very low scatter. In the following step, macro-paths and their corresponding trip lengths are estimated. Dynamic evolution of trip lengths is demonstrated using the present data, which is otherwise very difficult to capture with other types of data sources. Another important component calibrated is the time dependent path flow distribution between the different macro-paths for a given OD pair. The manuscript is concluded by presenting the time evolution of the User Equilibrium (UE) gap for different macroscopic OD pairs.

1 Introduction

Since the empirical existence of Macroscopic Fundamental Diagram (MFD) was first reported by Geroliminis and Daganzo (2008) for the city of Yokohama, Japan, several applications like traffic state estimation (Knoop and Hoogendoorn, 2014, Yildirimoglu and Geroliminis, 2014, Kavianipour *et al.*, 2019), perimeter control (Keyvan-Ekbatani *et al.*, 2012, Haddad and Mirkin, 2017, Ampountolas *et al.*, 2017, Mohajerpoor *et al.*, 2019), congestion pricing (Gu *et al.*, 2018) and cruising for parking (Cao and Menendez, 2015, Leclercq *et al.*, 2017), *etc.* were proposed based on MFD approach. The three main elements for any MFD-based models are the underlying MFD, the trip lengths for each macro-path and the path flow distribution. The present work addresses the calibration of all the stated elements from mobile phone data records.

The estimation of MFD for urban networks is far from trivial. There exists two main types of data sources to estimate empirical MFD namely, Loop Detector Data (LDD) and Floating Car Data (FCD). Wang *et al.* (2015), Ampountolas and Kouvelas (2015) used the LDD to estimate the empirical MFDs for the urban networks of Sendai, China and Chania, Greece, respectively. However, Buisson and Ladier (2009) demonstrated that the slope of MFD depends on the distance of loop-detectors to the downstream traffic signals. More recently, Shim *et al.* (2019) studied the bifurcations in empirical MFDs by estimating them using roadside detectors

and Alonso *et al.* (2019) analyzed the shape of empirical MFDs for the urban corridors using LDD. On the other hand, FCD is more attractive than its counterpart, as it provides vehicular trajectory data. Typically, FCD is provided by either Global Positioning System (GPS) or mobile phones. FCD was used to estimate empirical MFD (Geroliminis and Daganzo, 2008, Bazzani *et al.*, 2011, Tsubota *et al.*, 2014), traffic monitoring (Herrera *et al.*, 2010) or travel time estimation (Jie *et al.*, 2011). Beibei *et al.* (2016), Ambühl and Menendez (2016) estimated an empirical MFD by data fusion of both LCD and FCD. Most of the works that employ FCD use only the GPS data from taxis to estimate MFD, as the GPS data of private cars is not readily available. Hence, the penetration rate of taxis is an important factor to estimate the MFD accurately from FCD (Du *et al.*, 2016).

Another key ingredient of the MFD-based modeling framework is the set of macro-paths and their corresponding trip lengths. It is not trivial to estimate neither the macro-paths nor their trip lengths using LDD without any further equipment. On the other hand, FCD from taxis can be processed to obtain a distribution of trip lengths. However, FCD is generally sparse and it fails to capture the repetitive trips made by the frequent users/residents. The importance of estimation of accurate and reliable trip lengths in the context of MFD-based simulation was discussed in-detail in Batista *et al.* (2019) and it is as critical as the estimation of the MFD *per se* for the accurate resolution of traffic dynamics. Similarly, it is difficult to observe the path flow distributions along each macro-path with the existing LDD or FCD data sources. Most often path flow coefficients are estimated using Dynamic Traffic Assignment (DTA) with User Equilibrium (UE), Stochastic User Equilibrium (SUE) or Bounded Rational User Equilibrium (BRUE) equilibration (Batista *et al.*, 2019). However, recent studies show that route choice discipline may not valid for macro-paths for large-scale networks (Mariotte *et al.*, 2020). At the same time, there have not been any works proposed to estimate the path flow coefficient from the empirical data. These research gaps can be appropriately addressed by using massive phone data to calibrate the above discussed models.

The present work proposes a method to estimate the empirical MFD of any urban network from the Location Based Service (LBS) data. This type of data is generated by the smartphone Apps, which share their location data actively to the App developer. The major drawback of this data is the diversity of users providing GPS locations using different modes of transportation. Hence, it is important to pre-process the data to extract information on cars and taxis. Another important factor in the case of LBS data is the sampling rate, which can vary from a few seconds to a few minutes depending on the type of App being used. This work proposes a method to enhance the data with poor sampling rates to obtain accurate travel distance. This work also introduces a framework to estimate the time dependent penetration rates. The secondary contribution of this work is the analysis of trip lengths inside the network. A static and dynamic analysis of the trip lengths are elaborated in-detail. The final part of the manuscript discusses the estimation of path flow distribution. The proposed framework is generic and it can be used to process any type of phone data that has records of GPS coordinates and timestamps.

2 Data Description and Pre-processing

The data contains the positioning of the smartphone devices either by GPS or WiFi Positioning System (WPS) for the city of Dallas, Texas in the United States for a period of 2 months from March, 2017 to April, 2017. In the present work, downtown Dallas and neighboring suburbs as shown in Fig. 1a are considered to calibrate the MFD models. Fig. 1b shows the link level presentation of the area under consideration, which extends across 160 km^2 and contains 18 386 nodes and 48 287 links. The length of the road network is 4 800 km, which includes all types of roads. The raw data contains an anonymized user ID, timestamp, longitude, latitude and uncertainty of the location. The data consists of 3.7 million users and there are around 4.5 billion

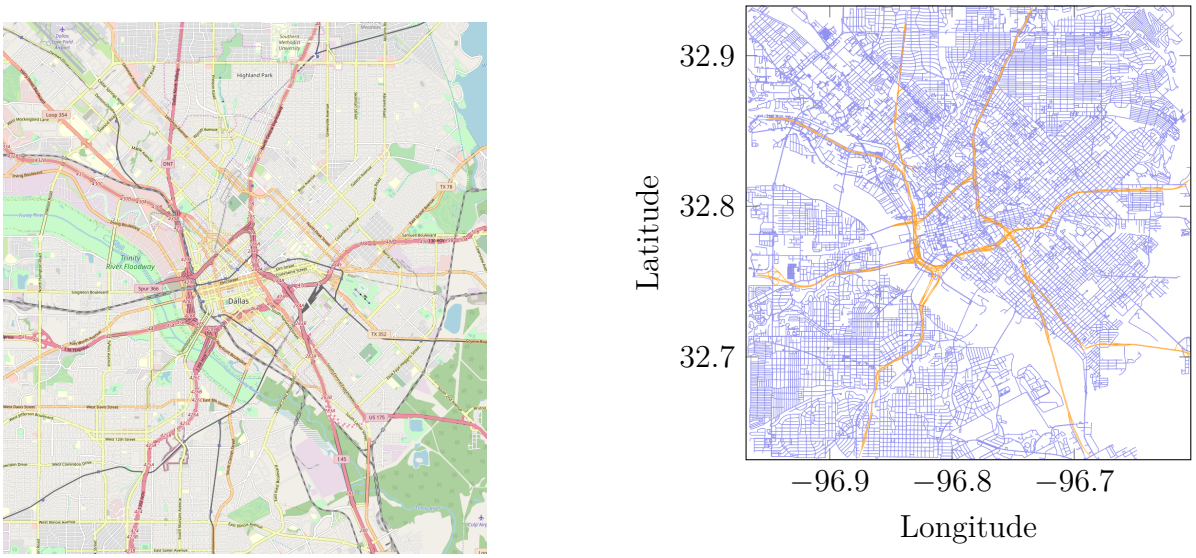

(a) Map of the Dallas, TX ©OpenStreetMap 2019.

(b) Link level representation of the Dallas.

Figure 1: Dallas network: map of the area and its link level description.

records available for processing. Data selection and segmentation of individual records into trips are discussed in-detail in Xu *et al.* (2019) and a similar approach is used in this work. The novelty of the present work in the data processing part is to use a computationally efficient map-matching technique to re-construct the trajectories with low sampling rate. This method is discussed in-detail in the following section.

3 Trip Enrichment Method

The main idea behind the enrichment method is to find the shortest path between the sparse records of a given trip. Two important tools are used in this context namely, OSMnx (Boeing, 2017), which is a Python package that is used to analyze the road networks and NetworkX (Hagberg *et al.*, 2008), another Python package used to study the dynamics of road networks. The enrichment method is explained with an example in the following.

Figure 2a shows three example traces of a sample trip with sparse records from the given data. All three trips have either 3 or 4 records for relatively long trips lengths of around 10 km. The result is a very poor resolution of the trajectory of the trip, which is shown in Fig. 2a. A simple Haversine distance between successive data points of each trip introduces a huge approximation in the traveled distances. At the same time, the traveled time estimation is unaffected due to the sparse records. The combination of these two phenomena can introduce a considerable scatter in the MFD and poor estimation of trip lengths. Hence, it is desirable to map the trajectory of the trip to the underlying road network as closely as possible.

In the current work, the trips are enriched using the spatial geometry of the network. For each trip, the distance between successive records is estimated. If the distance is bigger than a threshold, defined *a priori*, the location of the nearest nodes close to the GPS positions of those records is obtained. Once the locations of the nodes are obtained between the sparse data records, the shortest path between those two nodes is computed using NetworkX shortest path subroutine. The GPS locations of the nodes in the shortest path are added to the trip between those two sparse records. Fig. 2b presents the traces of considered trips after computing the shortest paths between the sparse records. It can be clearly noticed that the trajectory of each trip is matched to the network after the enrichment process.

Whenever the trace of the trip is enhanced between two sparse records, the timestamps are

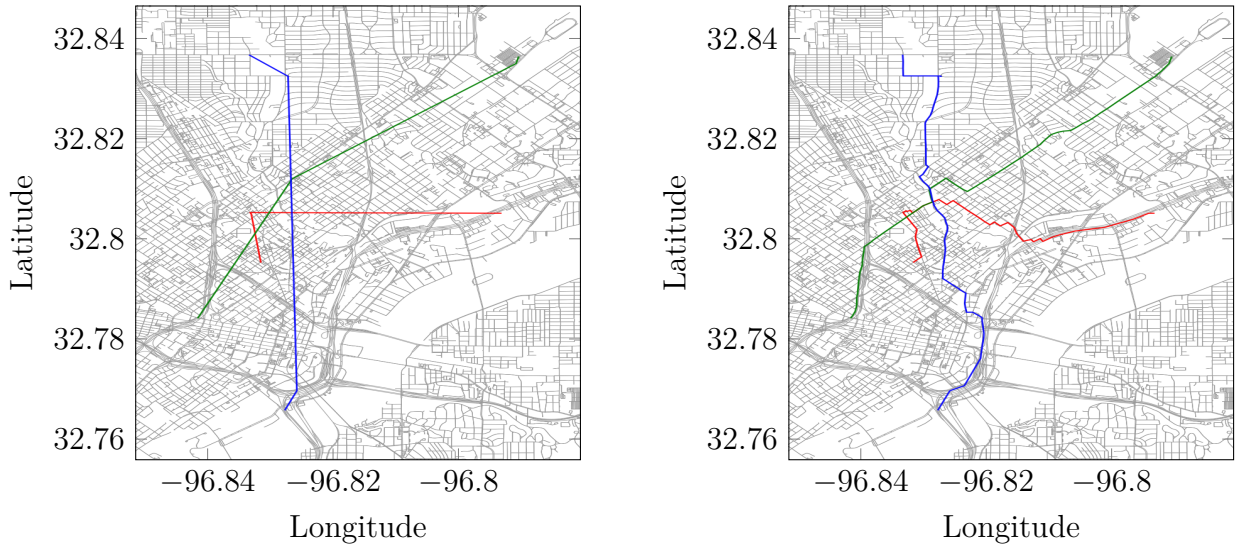

(a) Original traces of low resolution trips.

(b) Traces of the trips after enrichment method.

Figure 2: Trip enhancement method: Original and enriched traces.

also interpolated to match the spatial data. The timestamps are interpolated based on the average speed between the two records in the original trace. Hence, this method transforms the sparse spatial and temporal data into dense data, thereby improving the overall accuracy and the representation of the MFD.

4 Computation of Macroscopic Variables

4.1 Partitioning of the Network

Partitioning of the considered network into homogeneous reservoirs is the first step to estimate the macroscopic traffic variables. As the primary objective of the current work is to propose a methodology to estimate the MFD and the trip lengths from mobile phone data, a simple partitioning scheme is assumed. However, it is to be noted that the present framework can be used with any of the partitioning schemes proposed in the literature. The considered network is divided into 5 reservoirs as shown in Fig. 3a. The rationale behind the partitioning scheme is to have one reservoir for the downtown region and divide the region around the downtown into similar sized reservoirs. It is worth noting that the boundaries of reservoirs are not placed along with the road network, but in-between the road networks.

4.2 Estimation of Penetration Rates

Since the available mobile phone data accounts only for the part of the total traffic, it is necessary to estimate the penetration rate (ρ) of the vehicles to compute a well-defined MFD and path flow distributions. In this work, penetration rates are estimated by fusing the OD matrix data, LDD and LBS data. The OD matrix data is obtained from North Central Texas Council of Governments for the morning peak period, *i.e.*, 06:30 AM to 08:59 AM. Since this data does not have dynamic information of the OD matrix, LDD is used to transform this static OD matrix into a dynamic OD matrix. Fig. 3c presents the estimated normalized demand profile from the loop-detectors in the network. Now, using the OD matrix data for the given 2.5 h period and the normalized demand profile, it is possible to expand the partial OD matrix to a typical full day OD matrix. Table 1 gives the total number of vehicles for the

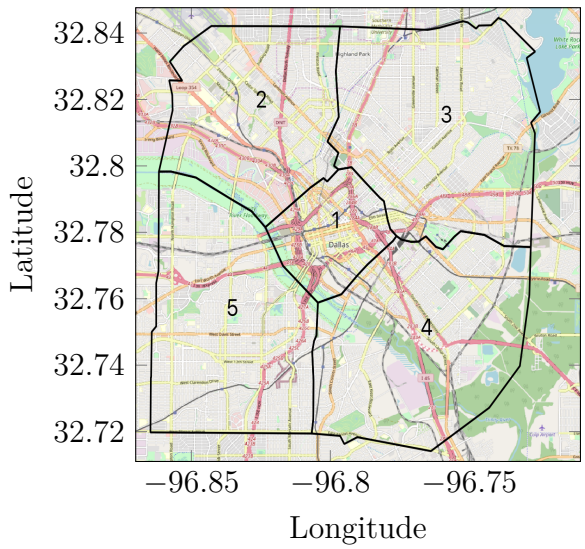

(a) Partitioning of Dallas network: Representation of the reservoirs along with their identities.

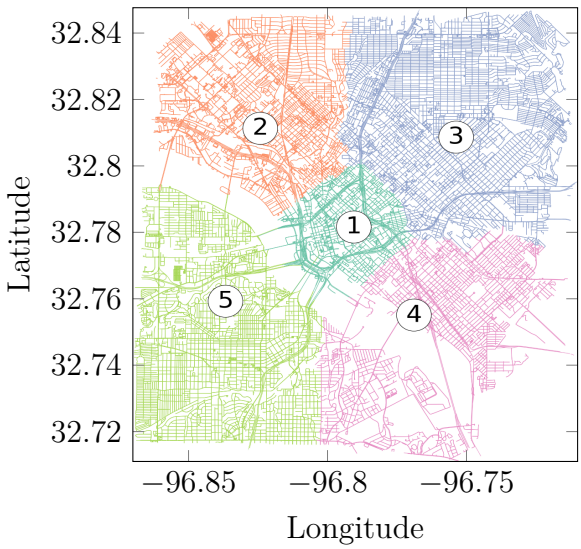

(b) Partitioning of Dallas network: Link level representation of the reservoirs.

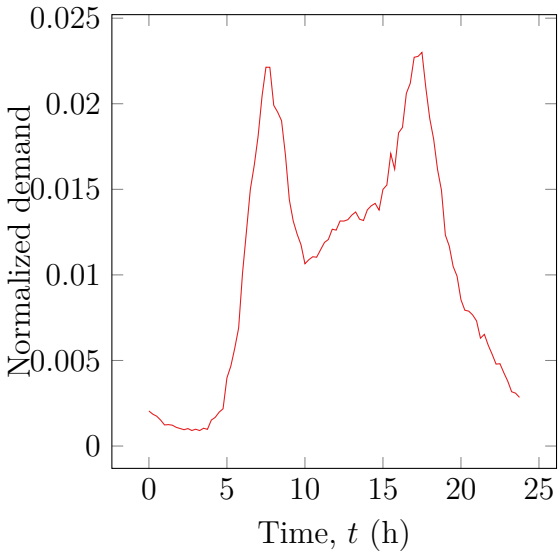

(c) Normalized demand profile for 24 h period.

Figure 3: Partitioning of Dallas network and normalized demand pattern for a typical day scenario.

Table 1: Total number of vehicles ($\times 10^4$) for 24 h period between different macroscopic OD pairs.

Reservoir	1	2	3	4	5
1	7.9	3.4	2.6	0.5	0.7
2	4.8	7.2	1.8	0.2	0.4
3	7.0	4.4	6.5	0.4	0.2
4	1.7	0.9	0.7	0.7	0.1
5	4.0	3.0	0.7	0.2	2.2

macroscopic OD pairs, *i.e.*, vehicle counts from one reservoir to another for 24 h period.

According to the generalized definitions of Edie (1963), the average network density (k) and flow (q) can be expressed as,

$$k = \frac{\sum_{i=1}^{N} TT_i}{L_n \, \Delta T} \text{ and } q = \frac{\sum_{i=1}^{N} TD_i}{L_n \, \Delta T}, \tag{1}$$

where TT_i and TD_i are time traveled and distance covered on a link l, respectively, L_n is the total network length, ΔT is the aggregation interval and N is the total number of links in the network under consideration. In the present work, an aggregation interval of 15 min is used. It is clear from eq. (1) that the density is computed using Total Traveled Time (TTT) and the flow is estimated by Total Traveled Distance (TTD) in the network by all vehicles within each aggregation interval. The density and flow of the network can be estimated using eq. (1) only if the trajectories of all the vehicles are known *a priori*. Often, that is not the case in reality and only trajectories of a fraction of the vehicles are available. Hence, it is necessary to correct the expressions in eq. (1) with penetration rates. According to Nagle and Gayah (2014), density and flow of vehicles in the network can be re-defined as,

$$k = \frac{\sum_{i=1}^{P} TT_i/\rho}{L_n \, \Delta T} \text{ and } q = \frac{\sum_{i=1}^{P} TD_i/\rho}{L_n \, \Delta T}, \tag{2}$$

where ρ is the penetration rate and it is defined as the number of probe vehicles to the total number of vehicles in the network. In eq. (2), the sum is made over the total number of probe vehicle trajectories P.

The final step to compute the macroscopic variables is to estimate the penetration rate. The current work proposes two different types of penetration rates namely, OD specific penetration rate (ρ_{od}) and origin specific penetration rate (ρ_o). It is possible to estimate the trip OD matrix for each day from the mobile phone data based on the departure time of each trip. Since the number of trips between the same OD can vary from day-to-day, trip OD matrix based on the mobile phone data is estimated for each day separately. Let $N^I_{od,p}$ be the number of trips from the data between origin o and destination d starting within the aggregation interval I. Similarly, $N^I_{od,n}$ is the total number of trips estimated by data fusion of loop detectors and OD matrix from NCTCOG as elaborated earlier within a given interval I. Now, OD specific penetration rate at the aggregation interval I can be defined as,

$$\rho^I_{od} = \frac{N^I_{od,p}}{N^I_{od,n}}. \tag{3}$$

Similarly, let $N^I_{o,p}$ be the total number of trips from the data originating from origin o to all the destinations for a given interval I. In the same way, $N^I_{o,n}$ is the total number of trips from

origin o to all the destinations computed from the NCTCOG data. Using these two quantities, origin specific penetration rate can be expressed as,

$$\rho_o^I = \frac{N_{o,p}^I}{N_{o,n}^I} \equiv \frac{\sum_{d=1}^{r} N_{od,p}^I}{\sum_{d=1}^{r} N_{od,n}^I}, \tag{4}$$

where r is the total number of macroscopic reservoirs in the network.

As the OD matrix provides the data of trip production to trip attraction, penetration rates should be used based on the departure time of the trip. Consider a trip i starting within an aggregation interval I between the OD pair od has traveled time and traveled distance of TT_i and TD_i, respectively. The expanded travel distance (TD_i^e) and the expanded travel time (TT_i^e) for the whole network considering the two types of penetration rates for that trajectory can be expressed as,

$$TT_i^{e,od} = \frac{TT_i}{\rho_{od}^{I_p}} \text{ and } TD_i^{e,od} = \frac{TD_i}{\rho_{od}^{I_p}}, \tag{5a}$$

$$TT_i^{e,o} = \frac{TT_i}{\rho_o^{I_p}} \text{ and } TD_i^{e,o} = \frac{TD_i}{\rho_o^{I_p}}, \tag{5b}$$

where suffixes/prefixes od and o represent that the expansion is done by OD and origin specific penetration factors, respectively and I_p is the aggregation interval corresponding to the departure time of trip i. Similarly, k and q can be expressed as,

$$k_{od} = \frac{\sum_{i=1}^{P} TT_i^{e,od}}{L_n\,\Delta T} \text{ and } q_{od} = \frac{\sum_{i=P}^{N} TD_i^{e,od}}{L_n\,\Delta T}, \tag{6a}$$

$$k_o = \frac{\sum_{i=1}^{P} TT_i^{e,o}}{L_n\,\Delta T} \text{ and } q_o = \frac{\sum_{i=P}^{N} TD_i^{e,o}}{L_n\,\Delta T}. \tag{6b}$$

5 Estimated MFDs

The average values of density and flow for each day are estimated using eqs. (6). Only data from the weekdays, which are 43 in total, is considered in the computation of the macroscopic variables to estimate a stable and reproducible MFD. One important factor to consider in this context is the phenomenon of hysteresis in the MFD for the urban networks (Leclercq and Paipuri, 2019). It is normal to observe the clockwise hysteresis loops in the MFD due to network heterogeneity, demand pattern, driver's behavior, *etc.* However, the loading of the network from near empty state, which is observed during late night hours, is more stable and reproducible. Hence, a parabolic curve is fitted for the estimated MFD for each weekday for the data point ranging from midnight till the morning peak hour, which is 08:00 AM in the present case. Only the days that show similar MFD fit characteristics are chosen to compute the mean MFD for each reservoir. In the present case, it is observed that on an average 18 days show similar MFD fits. Fig. 4 shows the estimated flow MFDs for the reservoirs, where the macroscopic variables are computed by the OD specific penetration rate. Firstly, it can be noticed that all the MFD curves are relatively stable with very little scatter. Reservoir 1 experiences the highest flow rate among all the reservoirs in the considered region, which corresponds to the downtown Dallas area. Another important inference to be made from the MFD plots is the presence of clockwise hysteresis loops in the MFDs. Reservoirs 1 and 3 in Figs. 4a and 4c, respectively exhibit clearer hysteresis during the morning peak hour compared to others. The hysteresis phenomenon is present in other reservoirs too, albeit the size of the loop is relatively smaller.

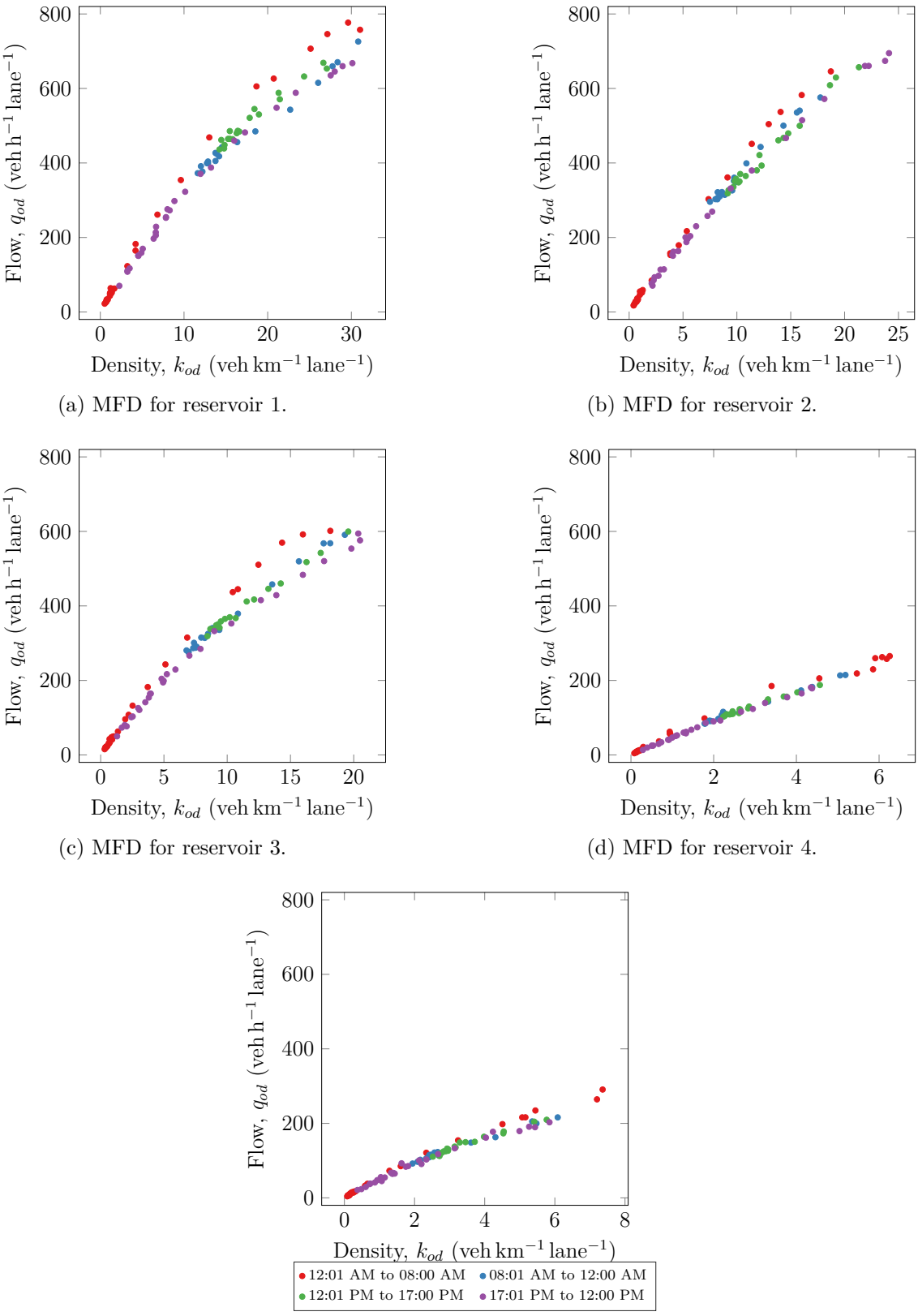

(a) MFD for reservoir 1.

(b) MFD for reservoir 2.

(c) MFD for reservoir 3.

(d) MFD for reservoir 4.

(e) MFD for reservoir 5.

Figure 4: Flow MFD estimates using the OD specific penetration rate for computing the density and the flow.

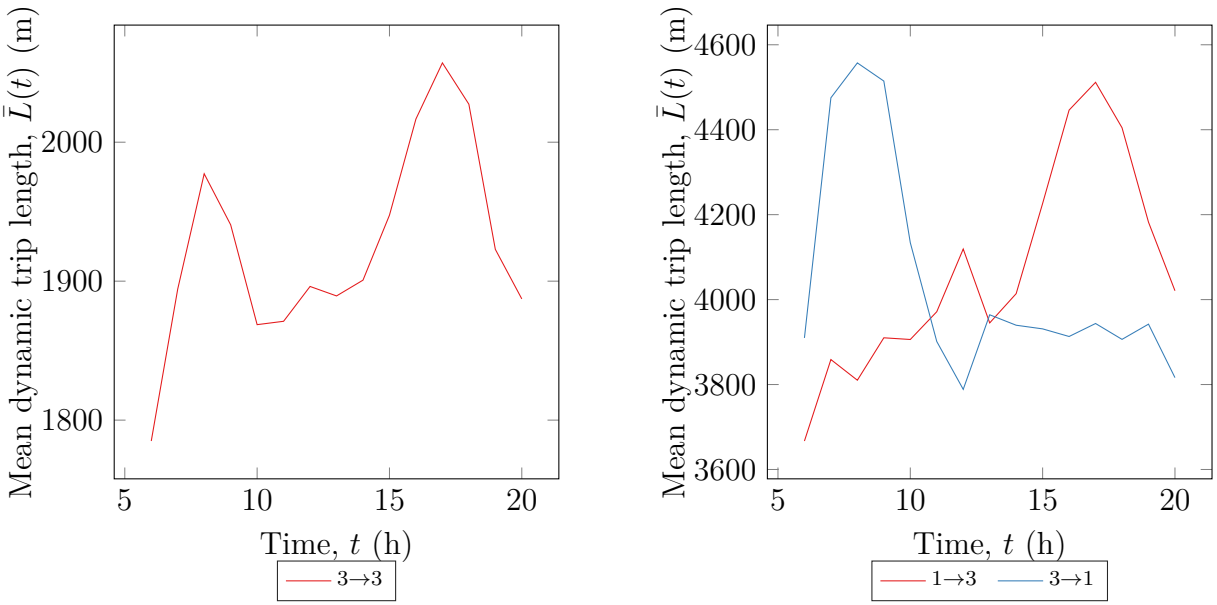

(a) Evolution of trip length for $3 \rightarrow 3$.

(b) Evolution of trip lengths for $1 \rightarrow 3$ and $3 \rightarrow 1$.

Figure 5: Mean dynamic trip lengths for different macro-paths.

6 Trip Lengths Estimation - Dynamic Analysis

There had not been many works on the dynamic variation of trip lengths using empirical data due to lack of data. The trip lengths within and between the reservoirs tend to be dynamic, where the users tend to prefer the alternative paths during the congestion periods. Batista *et al.* (2020) proposed a framework to estimate the dynamic trip lengths explicitly and concluded that including the dynamic changes in the trip lengths improves the accuracy of the MFD-based simulations. Note that in the present section, all the macro-paths are represented as the reservoir sequence. For instance, a trip that starts in reservoir 1 and ends in 3 by transversing through reservoir 2, it is named as $1 \rightarrow 2 \rightarrow 3$.

In the present work, the dynamic trip lengths between macroscopic OD pairs are estimated using the starting time of each trip. In order to do so, an aggregate time period of 60 min is considered. For a given OD pair, all the trips that are starting within a given aggregation period are selected and a mean trip length is estimated for that given period. Fig. 5 presents the mean evolution of the trip length for different macroscopic OD pairs. Consider Fig. 5a, where the evolution of internal macro-path $3 \rightarrow 3$ is presented. Two peaks, one at the morning peak hour and another at the evening peak hour, can be clearly noticed in the plot. This trend signifies that the users perhaps take the longer paths during peak hours to avoid the most used routes. Fig. 5b shows the dynamic trip lengths of the macro-paths $1 \rightarrow 3$ and $3 \rightarrow 1$. It is clear from the plots that the dynamic trip lengths evolution of the two macro-paths are nearly symmetric. This is due to the movement of the people from the suburban region to the downtown in the morning and *vice-versa* in the evening. It is difficult to predict these trends between different OD pairs *a priori* and appropriately calibrate the MFD models. This type of analysis has not been done before in the literature due to the lack of sufficient and reliable data. Therefore, this framework estimates the mean evolution of different macro-paths, which can be directly used in the MFD simulation framework.

The remaining work includes a deeper investigation of MFDs using two types of penetration rates presented. An analysis on speed MFDs will also be discussed. In addition, static analysis of the trip lengths, their distribution will be presented in-detail. Finally, the path flow coefficients are extracted from the data and corresponding empirical UE gaps are calibrated.

Acknowledgment

M. Paipuri and L. Leclercq acknowledge the funding from the European Research Council (ERC) under the European Union's Horizon 2020 research and innovation program (grant agreement No 646592 – MAGnUM project). Y. Xu and M. González acknowledge the support by the Berkeley Deep Drive (BDD) consortium.

References

Alonso, B., Á. Ibeas, G. Musolino, C. Rindone and A. Vitetta (2019). Effects of traffic control regulation on network macroscopic fundamental diagram: A statistical analysis of real data. *Transportation Research Part A: Policy and Practice*, *126*, 136 – 151.

Ambühl, L. and M. Menendez (2016). Data fusion algorithm for Macroscopic Fundamental Diagram estimation. *Transportation Research Part C: Emerging Technologies*, *71*, 184 – 197.

Ampountolas, K. and A. Kouvelas (2015). Real-time estimation of critical values of the macroscopic fundamental diagram for maximum network throughput. In *Transportation Research Board 94th Annual Meeting Transportation Research Board*, 15-1779. Washington.

Ampountolas, K., N. Zheng and N. Geroliminis (2017). Macroscopic modelling and robust control of bi-modal multi-region urban road networks. *Transportation Research Part B: Methodological*, *104*, 616 – 637.

Batista, S. F. A., L. Leclercq and M. Menendez (2020). Regional dynamic traffic assignment framework with time-dependent trip lengths. In *Transportation Research Board 99th Annual Meeting Transportation Research Board*, 20-00615. Washington.

Batista, S.F.A., L. Leclercq and N. Geroliminis (2019). Estimation of regional trip length distributions for the calibration of the aggregated network traffic models. *Transportation Research Part B: Methodological*, *122*, 192 – 217.

Bazzani, A., B. Giorgini, R. Gallotti, L. Giovannini, M. Marchioni and S. Rambaldi (2011). Towards congestion detection in transportation networks using GPS data. In *2011 IEEE Third International Conference on Privacy, Security, Risk and Trust and 2011 IEEE Third International Conference on Social Computing*, pages 1455–1459.

Beibei, J. Y., H. J. van Zuylen and L. Shoufeng (2016). Determining the Macroscopic Fundamental Diagram on the basis of mixed and incomplete traffic data. In *Transportation Research Board 95th Annual Meeting Transportation Research Board*, 16-2601. Washington.

Boeing, G. (2017). OSMnx: New methods for acquiring, constructing, analyzing, and visualizing complex street networks. *Computers, Environment and Urban Systems*, *65*, 126 – 139.

Buisson, C. and C. Ladier (2009). Exploring the impact of homogeneity of traffic measurements on the existence of Macroscopic Fundamental Diagrams. *Transportation Research Record: Journal of the Transportation Research Board*, *2124*, 127–136.

Cao, J. and M. Menendez (2015). System dynamics of urban traffic based on its parking-related-states. *Transportation Research Part B: Methodological*, *81*, 718 – 736. ISTTT 21 for the year 2015.

Du, J., H. Rakha and V. V. Gayah (2016). Deriving Macroscopic Fundamental Diagrams from probe data: Issues and proposed solutions. *Transportation Research Part C: Emerging Technologies*, *66*, 136 – 149. Advanced Network Traffic Management: From dynamic state estimation to traffic control.

Edie, L. C. (1963). Discussion of traffic stream measurements and definitions. In *The 2nd International Symposium on Theory of Traffic flow*, 139–154. London.

Geroliminis, N. and C. F. Daganzo (2008). Existence of urban-scale macroscopic fundamental diagrams: Some experimental findings. *Transportation Research Part B: Methodological*, *42*(9), 759 – 770.

Gu, Z., S. Shafiei, Z. Liu and M. Saberi (2018). Optimal distance- and time-dependent area-based pricing with the Network Fundamental Diagram. *Transportation Research Part C: Emerging Technologies*, *95*, 1 – 28.

Haddad, J. and B. Mirkin (2017). Coordinated distributed adaptive perimeter control for large-scale urban road networks. *Transportation Research Part C: Emerging Technologies*, *77*, 495 – 515.

Hagberg, A., P. Swart and D. S Chult (2008). Exploring network structure, dynamics, and function using NetworkX.

Herrera, J. C., D. B. Work, R. Herring, X. (Jeff) Ban, Q. Jacobson and A. M. Bayen (2010). Evaluation of traffic data obtained via gps-enabled mobile phones: The mobile century field experiment. *Transportation Research Part C: Emerging Technologies*, *18*(4), 568 – 583.

Jie, L., H. van Zuylen, L. Chunhua and L. Shoufeng (2011). Monitoring travel times in an urban network using video, GPS and bluetooth. *Procedia - Social and Behavioral Sciences*, *20*, 630 – 637. The State of the Art in the European Quantitative Oriented Transportation and Logistics Research – 14th Euro Working Group on Transportation & 26th Mini Euro Conference & 1st European Scientific Conference on Air Transport.

Kavianipour, M., R. Saedi, A. Zockaie and M. Saberi (2019). Traffic state estimation in heterogeneous networks with stochastic demand and supply: Mixed lagrangian–eulerian approach. *Transportation Research Record*, *0*(0), 0361198119850472. (In press).

Keyvan-Ekbatani, M., A. Kouvelas, I. Papamichail and M. Papageorgiou (2012). Exploiting the fundamental diagram of urban networks for feedback-based gating. *Transportation Research Part B: Methodological*, *46*(10), 1393 – 1403.

Knoop, V. L. and S. P. Hoogendoorn (2014). Network transmission model: a dynamic traffic model at network level. In *Transportation Research Board 93rd Annual Meeting Transportation Research Board*, 14-1104. Washington.

Leclercq, L. and M. Paipuri (2019). Macroscopic traffic dynamics under fast-varying demand. *Transportation Science*, *53*(6), 1526–1545.

Leclercq, L., A. Sénécat and G. Mariotte (2017). Dynamic macroscopic simulation of on-street parking search: A trip-based approach. *Transportation Research Part B: Methodological*, *101*, 268 – 282.

Mariotte, G., L. Leclercq, S. Batista, J. Krug and M. Paipuri (2020). Calibration and validation of multi-reservoir mfd models: A case study in lyon. *Transportation Research Part B: Methodological*. (Under Review).

Mohajerpoor, R., M. Saberi, H. L. Vu, T. M. Garoni and M. Ramezani (2019). H_∞ robust perimeter flow control in urban networks with partial information feedback. *Transportation Research Part B: Methodological*. (In press).

Nagle, A. S. and V. V. Gayah (2014). Accuracy of networkwide traffic states estimated from mobile probe data. *Transportation Research Record*, *2421*(1), 1–11.

Shim, J., J. Yeo, S. Lee, S. H. Hamdar and K. Jang (2019). Empirical evaluation of influential factors on bifurcation in macroscopic fundamental diagrams. *Transportation Research Part C: Emerging Technologies*, *102*, 509 – 520.

Tsubota, T., A. Bhaskar and E. Chung (2014). Macroscopic Fundamental Diagram for Brisbane, Australia: Empirical findings on network partitioning and incident detection. *Transportation Research Record*, *2421*(1), 12–21.

Wang, P., K. Wada, T. Akamatsu and Y. Hara (2015). An empirical analysis of macroscopic fundamental diagrams for sendai road networks. *Interdisciplinary Information Sciences*, *21*(1), 49–61.

Xu, Y., R. Di Clemente and M. C. Gonzalez (2019). Understanding route choice behavior with location-based services data. (In preparation).

Yildirimoglu, M. and N. Geroliminis (2014). Approximating dynamic equilibrium conditions with macroscopic fundamental diagrams. *Transportation Research Part B: Methodological*, *70*, 186 – 200.